JOURNAL OF GEOPHYSICAL RESEARCH, VOL. 113, D23212, doi:10.1029/2008JD010620, 2008

Click Here for Full Article

Long-range transport and vertical structure of Asian dust from CALIPSO and surface measurements during PACDEX

Jianping Huang,[1] Patrick Minnis,[2] Bin Chen,[1] Zhongwei Huang,[1] Zhaoyan Liu,[3] Qingyun Zhao,[4] Yuhong Yi,[5] and J. Kirk Ayers[5]

Received 17 June 2008; revised 12 September 2008; accepted 29 September 2008; published 11 December 2008.

[1] Knowledge of long-range transport and vertical distribution of Asian dust aerosols in the free troposphere is important for estimating their impact on climate. Cloud-Aerosol Lidar and Infrared Pathfinder Satellite Observations (CALIPSO), surface micropulse lidar (MPL), and standard surface measurements are used to directly observe the long-range transport and vertical distribution of Asian dust aerosols in the free troposphere during the Pacific Dust Experiment (PACDEX). The MPL measurements were made at the Loess Plateau (35.95°N, 104.1°E) near the major dust source regions of the Taklamakan and Gobi deserts. Dust events are more frequent in the Taklamakan, where floating dust dominates, while more intensive, less frequent dust storms are more common in the Gobi region. The vertical distribution of the CALIPSO backscattering/depolarization ratios indicate that nonspherically shaped dust aerosols floated from near the ground to an altitude of approximately 9 km around the source regions. This suggests the possible long-range transport of entrained dust aerosols via upper tropospheric westerly jets. A very distinct large depolarization layer was also identified between 8 and 10 km over eastern China and the western Pacific Ocean corresponding to dust aerosols transported from the Taklamakan and Gobi areas, as confirmed by back trajectory analyses. The combination of these dust sources results in a two-layer or multilayered dust structure over eastern China and the western Pacific Ocean.

Citation: Huang, J., P. Minnis, B. Chen, Z. Huang, Z. Liu, Q. Zhao, Y. Yi, and J. K. Ayers (2008), Long-range transport and vertical structure of Asian dust from CALIPSO and surface measurements during PACDEX, *J. Geophys. Res.*, *113*, D23212, doi:10.1029/2008JD010620.

1. Introduction

[2] Recently, special attention has been dedicated to understanding the effect of dust aerosols on regional and global climates. The impact of long-range transport of dust and air pollution from their continental sources over oceanic regions is one of the outstanding problems in understanding regional and global climate change. Dust mixed with air pollution leads to a brownish haze, which absorbs and scatters sunlight, leading to a large reduction of sunlight at the surface [*Ramanathan et al.*, 2001], the so-called "global dimming." The vertical structure and degree of vertical mixing between dust and pollution layers during transport are poorly understood, primarily because of the lack of high-resolution observations. Seasonal mean sunlight reductions can be as large as 10–15% over large portions of, if not entire, ocean basins. Because of the fast large-scale transport in the upper troposphere, aerosols such as dust and black carbon, once they enter the upper troposphere (above ~8 km), can be transported around the earth in a latitudinal belt in a week or two. As a result, dust from Asia can influence upper tropospheric clouds over North America and the Atlantic, just as Saharan dust affects clouds over North America. For example, *DeMott et al.* [2003] analyzed in situ data collected during a field experiment and concluded that fine dust from North Africa contributed significantly to ice nuclei populations over Florida. Using ground-based lidar polarization data, *Sassen* [2002] deduced that Asian dust affected the formation and phase of clouds, leading to unusually warm cirrus ice clouds. Dust aerosols generated in the Taklamakan and Gobi areas are usually transported eastward by the prevailing westerlies and can pass over China, North and South Korea, and Japan, [*Iwasaka et al.*, 1983; *Zhang et al.*, 1997; *Murayama et al.*, 2001; *Uno et al.*, 2001; *Natsagdorj et al.*, 2003] and sometimes are carried farther across the Pacific Ocean reaching North America [*Uno et al.*, 2001; *Husar et al.*, 2001; *Sassen*, 2002]. Additional exploration and study are required to fully understand the mechanisms and extent of long-range transport of Asian dust. The Cloud-Aerosol Lidar and Infrared Pathfinder Satellite Observations (CALIPSO) satellite supplies a wealth of actively sensed

[1]College of Atmospheric Science, Lanzhou University, Lanzhou, China.
[2]NASA Langley Research Center, Hampton, Virginia, USA.
[3]National Institute of Aerospace, Hampton, Virginia, USA.
[4]Gansu Meteorological Bureau, Lanzhou, China.
[5]Science Systems and Applications Incorporated, Hampton, Virginia, USA.

Copyright 2008 by the American Geophysical Union.
0148-0227/08/2008JD010620$09.00

data over the region and provides an outstanding opportunity for studying dust vertical structure and long-range transport.

[3] The vertical distribution of dust aerosols is another critical factor impacting the effects of dust on radiative forcing and climate [*Claquin et al.*, 1998; *Zhu et al.*, 2007; *Forster et al.*, 2007]. An analysis of observations by *Minnis and Cox* [1978] and a model study by *Carlson and Benjamin* [1980] showed that an elevated Saharan dust layer could change the atmospheric heating rate dramatically. *Liao and Seinfeld* [1998] claimed that clear-sky longwave radiative forcing and cloudy sky top-of-atmosphere (TOA) shortwave (SW) radiative forcing are very sensitive to the dust layer altitude. *Meloni et al.* [2005] found that SW aerosol radiative forcing at the TOA has a strong dependence on aerosol vertical profiles. Numerous observations [*Sasano*, 1996; *Liu et al.*, 2002; *Zhou et al.*, 2002; *Murayama et al.*, 2001, 2004; *Shimizu et al.*, 2004] over eastern Asia have shown elevated dust plumes lofted into the free troposphere during spring. *Kwon et al.* [1997] revealed that air masses between 2 and 4 km mainly come from the Gobi Desert, while air parcels between 4 and 7 km originate from the region near the Taklamakan Desert. On the basis of aircraft observations, ground-based lidar measurements, and backward trajectory analysis, *Matsuki et al.* [2003] confirmed that the Taklamakan Desert is an important source for the background dust in the upper troposphere above 4 km. Airborne measurements taken during ACE-Asia also detected multiple aerosol layers near Tokyo [*Murayama et al.*, 2003]. Recently, *Uno et al.* [2008] reported the three-dimensional structure of Asian dust outflow from a dust source region to the northwestern Pacific Ocean. They found that the elevated dust was transported to the Pacific Ocean with the major dust layer maintaining a height between 2.5–4.0 km, with a potential temperature of 302–306 K.

[4] Prior to the availability of actively sensed data, aerosols were measured in situ and with passive radiometers at only selected sites around the globe. The in situ method consists of collecting aerosol samples on filters and chemically analyzing them to obtain the mass concentration of different aerosol species. These are then converted to number distribution and subsequently to optical depths using Mie scattering theory [*Satheesh and Ramanathan*, 2000]. Radiometric surface measurements of aerosol optical depth (AOD) at visible and near-infrared wavelengths use an automatic sun tracking photometer (CE318, Cimel). The measured surface-reaching solar spectral radiances are converted to optical depth on the basis of their ratios to radiances at the top of the atmosphere (TOA) [*Holben et al.*, 1998]. Aerosol properties measured in situ at the surface are converted to column values using assumptions about the vertical profiles. The surface aerosol properties are often quite different from the column aerosol properties because of the presence of distinct aerosol layers aloft [*Ramanathan et al.*, 2001]. Thus, the assumption that different days have the same aerosol vertical profile can result in large errors (up to a factor of two) [*Satheesh*, 2002]. Sun photometer measurements yield total column optical depth but provide no information about vertical structure. Shortcomings in these older measurement systems have been overcome in airborne, space-based (such as CALIPSO) and surface lidars that can accurately profile the physical properties of dust aerosols through the atmosphere enabling the reduction of uncertainties in the dust aerosol radiative forcing.

[5] The international Pacific Dust Experiment (PACDEX), conducted from March through May 2007, studied dust and pollution transport across the Pacific Ocean by taking intensive observations of dust plumes as they advected across the Pacific and into North America. An important part of PACDEX is understanding where the dust was generated and how it reached the Pacific. This paper examines the long-range transport and vertical distribution of Asian dust over the source regions and into the Pacific Ocean troposphere using combined CALIPSO and surface measurements. Unlike most space-based remote sensing instruments, CALIPSO can observe aerosols and their vertical structure over bright surfaces and beneath thin clouds as well as in clear sky conditions [*Winker et al.*, 2007; *Hu et al.*, 2006; *D. Liu et al.*, 2008; *Z. Liu et al.*, 2006, 2008; *Vaughan et al.*, 2004; *Huang et al.*, 2007]. However, the CALIPSO measurements need to be validated by using surface lidar as well as other in situ or surface instruments to assess the accuracy of the retrievals. To date only a few studies comparing ground-based lidar and CALIPSO measurements over east Asia have been attempted and quantitative analyses of the vertical structure of Asian dust related to lidar observations are rather scarce. The CALIPSO measurements, used in conjunction with surface observations, should lead to reliable analyses of Asian dust long-range transport and vertical structure, and expand the understanding of their impact on climate.

2. Satellite and Surface Data

2.1. CALIPSO Data

[6] The CALIPSO Cloud-Aerosol Lidar with Orthogonal Polarization (CALIOP) instrument measures vertical profiles of elastic backscatter at 532 and 1064 nm near nadir during both day and night phases of the orbit. In addition to total backscatter at both wavelengths, CALIOP provides profiles of linear depolarization at 532 nm. The depolarization measurements enable discrimination between ice and water clouds and identification of nonspherical aerosol particles. The primary products are three calibrated and geolocated lidar profiles of 532- and 1064-nm total attenuated backscatters and a 532-nm depolarization ratio, which is computed from the two polarization components of the attenuated backscatter. The CALIPSO level 2 data products (version 1.10) contain the cloud and aerosol layer and column properties. Level 1B data are first averaged into 5-km cloud layer products that are used to screen out cloudy profiles [*D. Liu et al.*, 2008].

[7] Dust aerosols can be identified in a given altitude range of a lidar profile using the volume depolarization ratio (VDR), defined as the ratio of the perpendicular to parallel components of received lidar signals (including both particulate and molecular scattering) at 532 nm. The dust depolarization ratio is high because of the nonsphericity of the particles. Conversely, the depolarization ratio is low (close to zero) for other types of aerosols. Therefore, the depolarization ratio is normally used as an indicator to separate dust from other aerosol types [*Murayama et al.*, 2001]. A threshold of 0.06 is used to detect the dust layer [*D. Liu et al.*, 2008]. This value corresponds to a horizontal

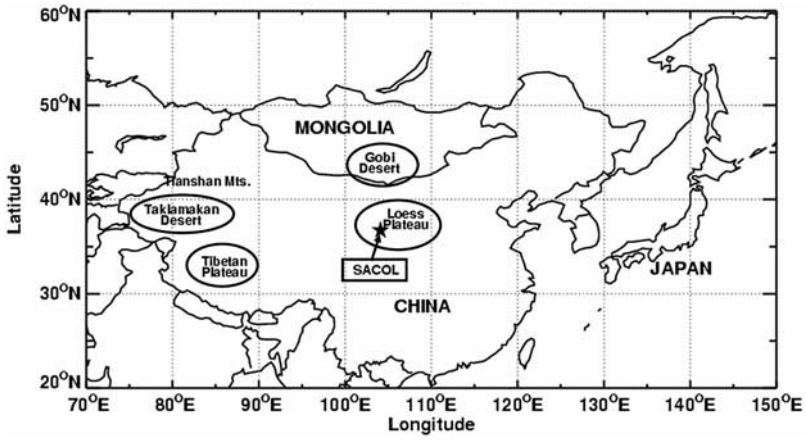

Figure 1. Location of Lanzhou University Semi-Arid Climate and Environment Observatory (SACOL).

visibility exceeding 30 km at a 1-km altitude for a dust layer having a particulate depolarization ratio (PDR) of 0.35 and a lidar ratio of 45 sr. Thus, all normally defined dust events, including dust storm (visibility <1 km), blowing dust (1–10 km), and floating dust (<10 km) will likely be detected with this threshold. *Z. Liu et al.* [2008] provide a detailed description of the data processing.

2.2. Surface Micropulse Lidar

[8] The Micropulse Lidar (MPL) Network (MPLnet) lidar [*Welton et al.*, 2001] was installed during April 2007 at the Lanzhou University Semi-Arid Climate and Environment Observatory (SACOL) [*Huang et al.*, 2008], located at 35.95°N, 104.1°E on the Loess Plateau in northwestern China (Figure 1). It provided real-time backscatter vertical profile images during PACDEX. The MPL system employs an optical transceiver that consists of a pulsating 527-nm Nd:YAG/Nd:YLF laser, an Avalanche Photo Diode (APD) photon counting detector, a signal processing unit, and a data processor. The laser pulse duration is 100 ns, yielding a vertical resolution of 75 m. The range-corrected, normalized lidar return signal for one transmitted laser pulse is a combination of the backscatter energy from Rayleigh and aerosol components. The color maps in this article plot the backscatter intensity after the range, overlap, and Rayleigh corrections have been applied, and represent only the aerosol backscatter intensity as a function of altitude. An AERONET-Cimel Sun photometer [*Holben et al.*, 1998]

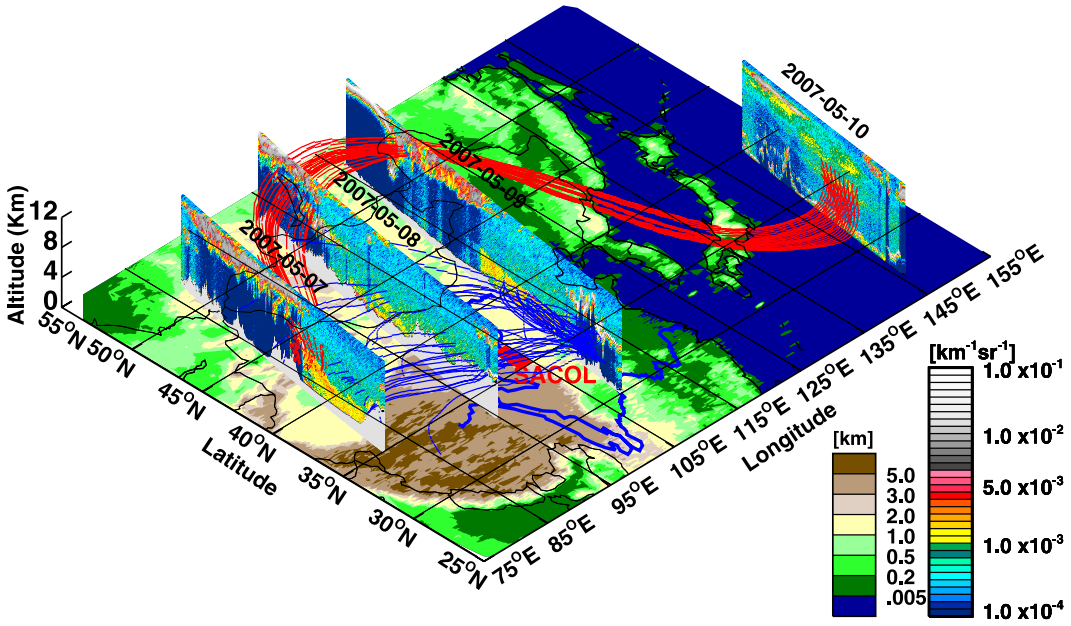

Figure 2. Illustration of first dust event, which originated in the Taklamakan Desert on 7 May 2007 and was transported to the Pacific Ocean. Red lines represent back trajectories initialized over the western Pacific. Blue lines represent back trajectories initialized over central China. The vertical images (curtain files) show the CALIPSO 532-nm total attenuated backscatter. The color scales on the left represent topographical elevation, and those on the right represent the 532-nm total attenuated backscatter (km^{-1} sr^{-1}).

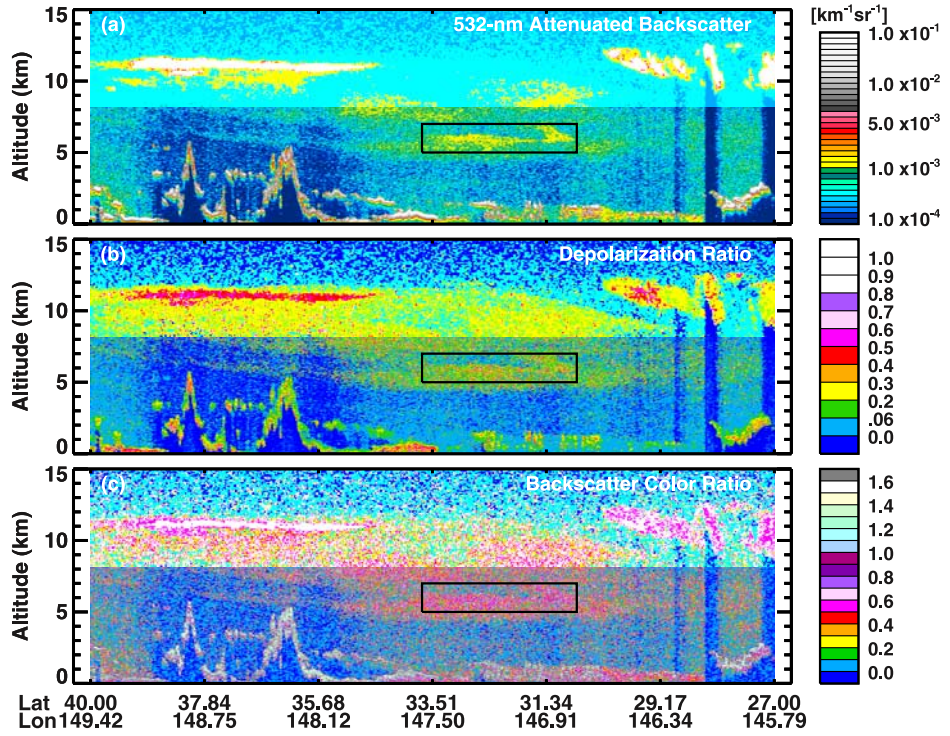

Figure 3. CALIPSO altitude-orbit cross-section measurements of (a) 532-nm total attenuated backscatter intensity (km^{-1} sr^{-1}), (b) volume depolarization ratio, and (c), 1064-nm/532-nm backscatter color ratio over the western Pacific Ocean for 10 May 2007. The black rectangle (Figure s 3a–3c) is the back trajectory initialization area.

was also deployed; its measurements can be compared with aerosol column-integrated features. Other surface measurements available from SACOL include (1) boundary layer meteorological parameters, (2) surface radiation, (3) surface fluxes, (4) soil heat and water moisture, (5) ambient air quality, (6) aerosol optical properties, (7) temperature and water vapor profiles, and (8) sky conditions. For additional information about the MPL and/or SACOL, visit the http://climate.lzu.edu.cn website.

2.3. Other Surface Observations

[9] Surface meteorological data were obtained from the Gansu Meteorological Bureau and include daily standard surface observations and daily charts. The Hybrid Single-Particle Lagrangian Integrated Trajectory (HYSPLIT) model [*Draxler and Rolph*, 2003] (http://www.arl.noaa.gov/ready/hysplit4.html) was used to compute back trajectories on the basis of winds from the National Center for Environmental Prediction (NCEP) analyses.

3. Case Study

[10] CALIPSO observations taken during 4 nights (7–10 May) over China and the Pacific, and back trajectories illustrate the time evolution and transport of the dust during the first event (Figure 2). The red lines in Figure 2, which originate in the western Pacific and extend northwestward to the Mongolia/Gobi desert area and then southwestward to the Xinjiang/Taklamakan desert area, represent 5000–7000 m back trajectories produced by the HYSPLIT model. The 4-day back trajectories were initialized on 10 May in the western Pacific. The blue lines represent 1500–3000 m back trajectories produced by HYSPLIT. They originate in central China and extend to the Taklamakan desert. The vertical images superimposed on the map show the CALIPSO 532-nm attenuated backscatter observations over the dust transport track. In these images, clouds appear as red, gray, or white and aerosols are shown in green, yellow, or orange [*Z. Liu et al.*, 2008]. The images from the CALIPSO observations coupled with the back trajectory analysis in Figure 2 indicate that the dust originated over the Taklamakan on 7 May 2007 (or perhaps somewhat earlier), and that that dust plume subsequently merged with extant dust over the

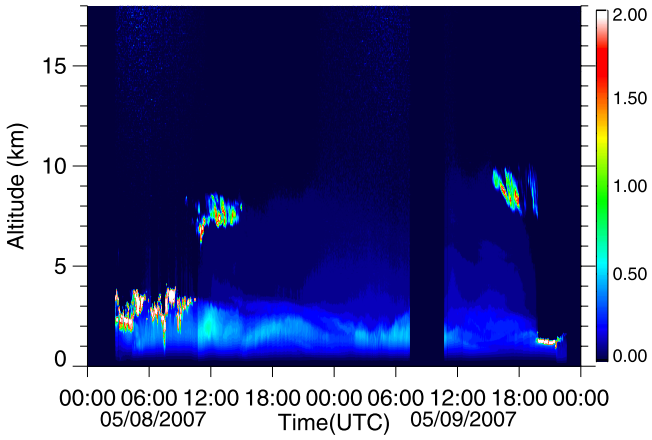

Figure 4. MPL normalized relative backscatter at SACOL for 8 and 9 May 2007.

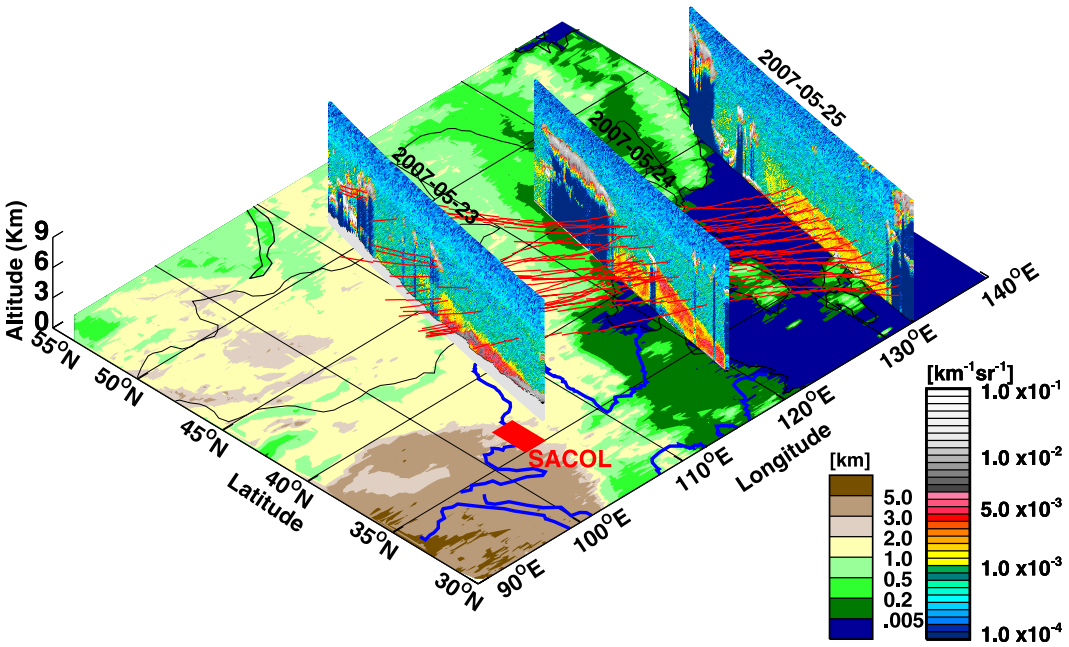

Figure 5. Illustration of second dust case event, which originated in the Gobi Desert on 23 May 2007 and was transported to the Sea of Japan. Red lines represent back trajectory analyses and show dust transport. Vertical images (curtain files) show the CALIPSO 532-nm total attenuated backscatter. The color scales on the left represent topographical elevation, and the color scales on the right represent 532-nm total attenuated backscatter.

Gobi Desert of Inner Mongolia and then advected over the Pacific (red lines in Figure 2). Figure 2 indicates that Taklamakan dust aerosols can also be transported to eastern China through alternative paths (blue lines in Figure 2). The paths at higher altitudes are dominated by the westerlies but lower-altitude trajectories are determined by regional weather systems and topography.

[11] Figure 3 shows plots of the 10 May 2007 attenuated backscatter at 532 nm, VDR, and backscatter color ratio (defined as the ratio of the 1064-nm to 532-nm attenuated backscatter) observed over the western Pacific. The back trajectory initialization region is denoted by the black rectangle. As discussed by *D. Liu et al.* [2008] and *Z. Liu et al.* [2008], dust aerosols have large VDR values and color ratios due to nonsphericity and to relatively large particle sizes, respectively. Other types of aerosols typically have small VDR values [*D. Liu et al.*, 2008; *Z. Liu et al.*, 2008]. For pollution aerosols, extinction at 532 nm is significantly (3–4 times) larger than at 1064 nm and the backscatter color ratio increases as the laser beam penetrates the polluted (black carbon enriched) aerosol layer from the top to base. The values of the three parameters plotted in Figure 3 indicate the presence of dust aerosols in the upper troposphere between 5∼10 km near the region marked by the rectangle. The back trajectory analyses confirm that these dust aerosols were transported from the Gobi/Taklamakan desert areas (red lines in Figure 2).

[12] Figure 4 shows normalized relative backscatter intensity as functions of UTC and altitude collected by the SACOL MPL during 8 and 9 May. The CALIPSO nadir track was 850 km east of SACOL on 8 May and 500 km west of SACOL on 9 May. During 8 May, strong aerosol backscatter was observed between 1 and 3 km with a light aerosol layer extending to 8 km after 1200 UTC. This aerosol layer persisted until 9 May (Figure 4b). A mixed aerosol-cloud layer between 7 and 8 km was also observed during both days. Although it is difficult to determine

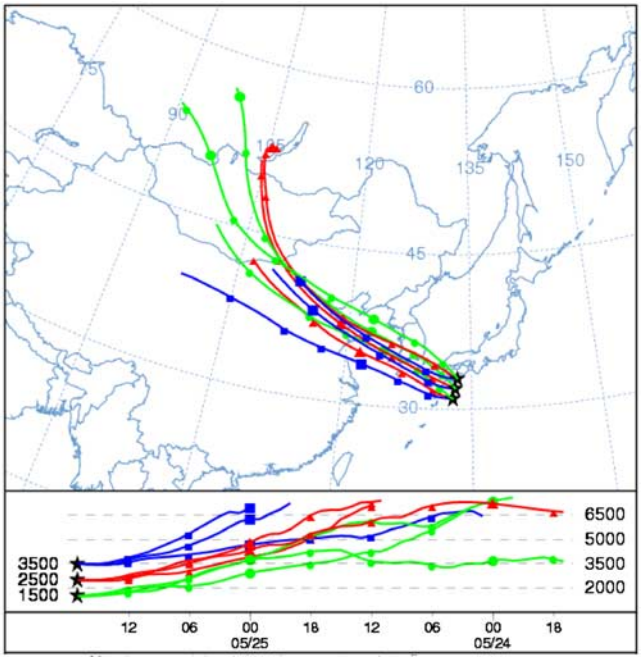

Figure 6. Back trajectory analyses, 1700 UTC, 25 May 2007, originating in the Sea of Japan, for three altitudes: 1500 m (green curves), 2500 m (red curves), and 3500 m (blue curves), produced with HYSPLIT. (top) Horizontal trajectory components and (bottom) vertical components.

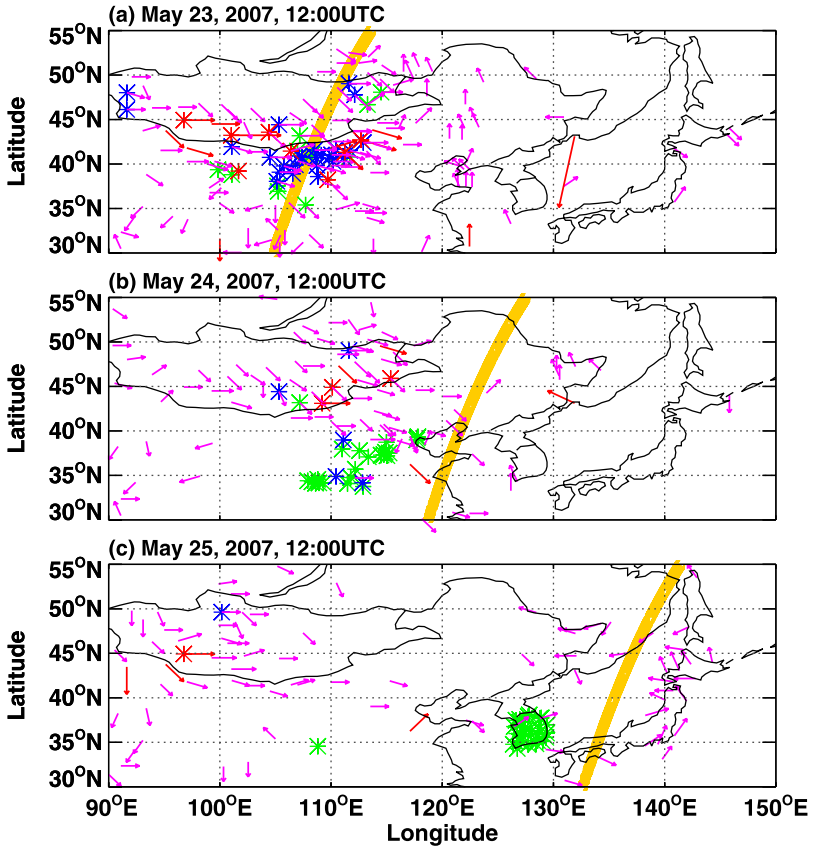

Figure 7. Surface station observations for (a) 23 May, (b) 24 May, and (c) 25 May. The red asterisk represents dust storms, blue asterisk denotes blowing dust, and green asterisk indicates floating dust. Short purple arrows indicate 7–12 m/s surface winds, long red arrows denote surface winds >13 m/s, and the yellow line shows CALIPSO nadir track.

whether the extended layer consists of dust aerosols, the back trajectories indicate that the air at this altitude originated in the Taklamakan region.

[13] The second dust storm, 23–25 May, originated in the Gobi Desert and was transported to the Pacific (Figure 5). The red lines represent the 1500–2500 m back trajectories that originate in the Sea of Japan and extend westward to the Gobi. The 3-day back trajectories were initialized on 25 May at the Korean Peninsula/Sea of Japan region. The nighttime CALIPSO observations in Figure 5 confirm that the dust event originated in the Gobi area. The back trajectories originated at three heights (1500, 2500 and 3500 m, AGL) and all pass over the eastern Gobi (Figure 6). Dust storms were first observed from Gobi ground stations at 0000 UTC, 23 May and persisted through 2000 UTC, 24 May. Figure 7 plots 3 days of ground station observations taken at 1200 UTC, about 4 h before the CALIPSO overpasses. On 23 May (Figure 7a,) the surface wind speeds over the Gobi area were generally between 7 and 12 m/s with some observations greater than 13 m/s. These wind speeds are sufficient to produce and support dust storm activity. Of the ground stations near the CALIPSO track, 11 reported floating dust with 24 and 7 reporting blowing dust and dust storms, respectively. On the second day (24 May), there were more than 22 ground stations near the CALIPSO track that recorded floating dust with 3 stations recording dust storms over the Gobi region. During the last day (25 May), 27 Korean Peninsula ground stations recorded floating dust. Unfortunately, confirmation of floating dust over Japan is not available because of lack of data.

[14] Figure 8 shows the CALIPSO measurements of attenuated backscatter, VDR, and color ratio for 23, 24 and 25 May 2007, respectively. The vertical distributions of attenuated backscatter in Figures 8a–8c reveal that the dust aerosols were distributed relatively uniformly from near the ground to an altitude of approximately 4–5 km. This uniformity suggests that the dust was well mixed and is consistent with the features of the large depolarization (Figures 8d–8h) and color ratios (Figures 8g–8i) of the aerosols. The MPL measurements taken at SACOL on 23 May (Figure 9), when the CALIPSO track was 240 km to the west, confirm that there was a uniform aerosol layer distributed from 1 to 5 km at night (1200–2400 UTC) with a light aerosol layer extending to 8 km near 1900 UTC, corresponding to the CALIPSO overpass.

[15] Few severe dust storms occurred over the study domain during PACDEX. Although both cases 1 and 2 are only light-to-moderate dust events, they still influenced a large area. Airborne dust was observed by CALIPSO in the free troposphere over eastern Asia and extended to the western Pacific Ocean in both cases. Back trajectory analyses indicate that airborne dust aerosols over the Pacific Ocean originated with dust activity in the Taklamakan and Gobi deserts, two of the most prolific and persistent dust

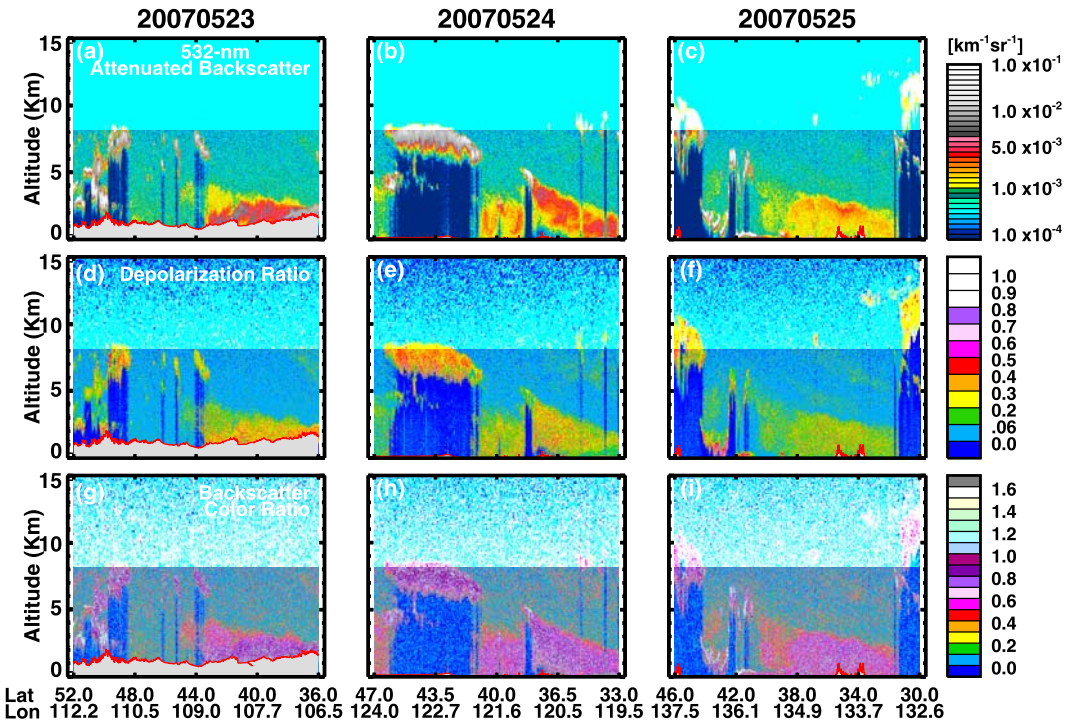

Figure 8. CALIPSO altitude-orbit cross-section measurements of (a–c) 532-nm total attenuated backscatter intensity (km^{-1} sr^{-1}), (d–f) volume depolarization ratio, and (g–i) 1064-nm/532-nm backscatter color ratio for 23 May (Figures 8a, 8d, and 8g), 24 May (Figures 8b, 8e, and 8h), and 25 May (Figures 8c, 8f, and 8i) over the dust event transport track shown in Figure 5.

sources in China [*Wang et al.*, 2005]. To determine if the long-range transport and vertical distribution seen for those two cases is representative of Asian dust transport in general, statistical results are presented in the following section.

4. Horizontal and Vertical Distribution

[16] The distribution of PACDEX (March to May) dust events shown in Figure 10 is based on 0600 UTC observations of dust events from 701 meteorological stations. Dust events are defined here as observations of floating dust (FD), blowing dust (BD) and dust storm (DS). In the FD category, dust particles are suspended in the air under calm or low-wind conditions, with horizontal visibility usually less than 10 km. In the BD category, dust and sand particles are physically lifted off the ground by winds, causing horizontal visibility to drop significantly (<10 km). In the DS category, sand and fine dust particles are frictionally lifted from the ground by strong winds (usually in excess of 5 m/s) under turbid atmospheric conditions. The horizontal visibility is reduced to less than 1 km. In the DS category, mechanically suspended particles can be transported over long distances in the upper atmosphere.

[17] As seen in Figure 10, the Taklamakan and Gobi deserts and surrounding areas are the two major Chinese dust source regions. The Taklamakan Desert has more significant dust outbreaks (>25 days in the period having dust activity) than the Gobi Desert (<10 days of dust). This distribution is similar to the 45-year mean distribution [*Wang et al.*, 2005]. As shown in Figures 2 and 5, dust aerosols from both the Taklamakan and Gobi deserts can be entrained to elevations above 5 km and transported over long distances by prevailing winds. Figure 11 shows the dust event frequency of occurrence for the three categories in three selected regions. It is obvious from Figure 11 that FD occurs much more frequently (91.1%) than BD and DS in the Taklamakan desert region (region A, Figure 10), but the FD percent (12.9%) is considerably smaller than BD and DS in the Gobi region (region B, Figure 10). More than 30% percent of the dust events that occur in the Gobi region are dust storms. In the Korea/Sea of Japan area (region C, Figure 10), FD is the only dust event. This is not surprising

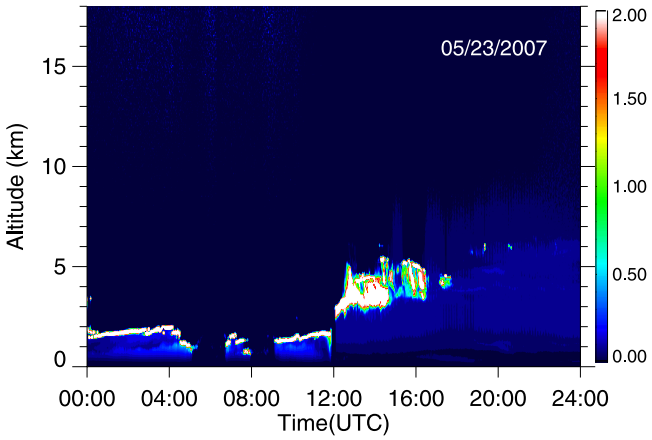

Figure 9. MPL normalized relative backscatter intensity at SACOL for 23 May 2007.

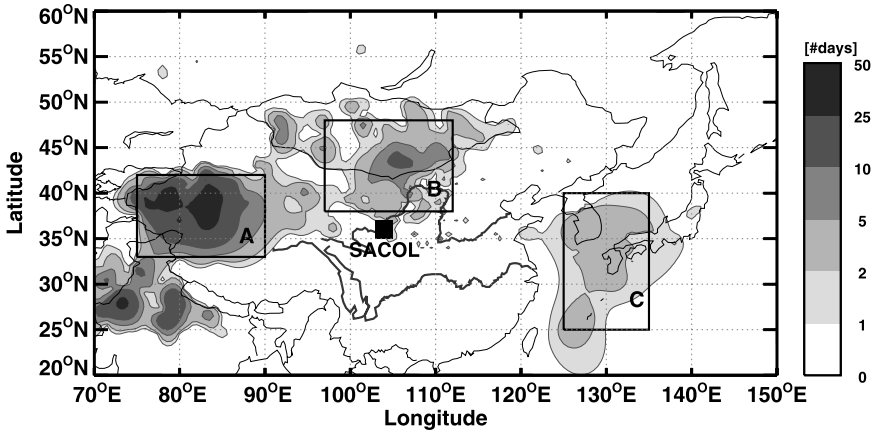

Figure 10. Distribution of surface-observed occurrence of dust storm (DS), blowing dust (BD), and floating dust (FD). Black boxes show regions selected for further analysis.

because all of the dust events that occurred in region C originated far to the west. This is the reason that most ground stations missed the transported and lofted dust aerosols, although CALIOP clearly observed the dust aerosols. Ground stations observe significantly fewer dust events than CALIPSO measurements [*Huang et al.*, 2007].

[18] On the basis of the first year of CALIPSO measurements (June 2006 to May 2007), *D. Liu et al.* [2008] studied the height-resolved global distribution of dust aerosols. They found that dust aerosols, which include DS, BD, FD, and even optically thin dust layers, can be effectively separated from other types of aerosols with a VDR threshold of 0.06 for 1 km layer average depolarization. This study uses the *D. Liu et al.* [2008] dust selection procedure and definition of frequency of dust aerosol occurrence (OCC), i.e.,

$$OCC_{\mathrm{i}} = N_{i,dust}/N_{cf} \tag{1}$$

where, $N_{i,dust}$ and N_{cf} are the number of dusty profiles in the vertical range (i) and the number of cloud-free profiles, respectively, in a $1^\circ \times 1^\circ$ grid box.

[19] Figure 12 shows the CALIPSO-derived vertical structure of dust occurrence at the Taklamakan (80°E), Gobi (102°E), east China (124°E), Japan/China Yellow Sea (146°E), and the Pacific Ocean (168°E) superimposed on a regional map. It shows that heavy dust layers are confined between 36°N and 42°N over the Taklamakan region. Dense dust aerosol layers can be found as high as 5 km. The Taklamakan is located in a basin surrounded by high mountains (the Tianshan Mts. to the north and the Kunlun Mts. to the south/southwest) that help to create and enhance circulations in the basin that are favorable for dust to remain suspended in the air for a long time [*Tsunematsu et al.*, 2005]. Figure 12 shows much less frequent dust over the Gobi Desert, especially for the portion located in southern Mongolia, as compared to the Tarim Basin area. Over the Gobi Desert, Figure 12 shows a uniform dust occurrence vertical structure with the highest dust layer at 10.5 km. Over eastern China, it shows a two-layer structure that may be associated with contributions from two major dust sources. Although there is a two-layer dust frequency structure over the Japan/China Yellow Sea area, the dust occurs at altitudes much lower than over eastern China. Dense dust occurred between 8 and 10 km over the Pacific, which is similar to that observed in the upper troposphere over eastern China and the Japan/China Yellow Sea area. Figure 12 clearly shows that dust aerosols generated in the Taklamakan/Gobi regions are transported across the Pacific Ocean via the westerly jet above 6 km. The dust frequency normally decreases with distance from the source region because of deposition and dispersion. This decrease in frequency is confirmed in Figure 13, which shows more dust in the upper than in the lower troposphere over the Pacific Ocean.

[20] Figure 14 shows nighttime mean profiles of the 532- and 1064-nm extinction coefficients for dust plumes over three selected areas (see Figure 10). A dust plume is defined as the thickness of a dust aerosol layer exceeding 0.9 km (i.e., there is at least a 0.9 km thick layer with VDR > 0.06 for the entire layer). There are significant differences in vertical structure between the profiles from different areas. Over the

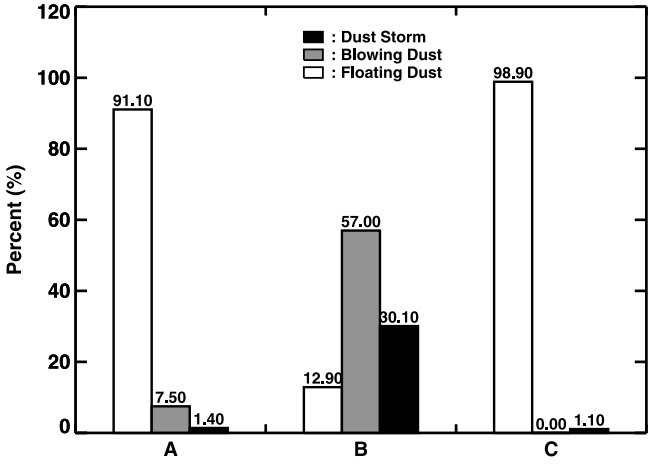

Figure 11. Dust event category frequency of occurrence for the selected regions. Dust storms (DS) are shown as solid bars, blowing dust (BD) is shown as shaded bars, and floating dust (FD) is shown as open bars.

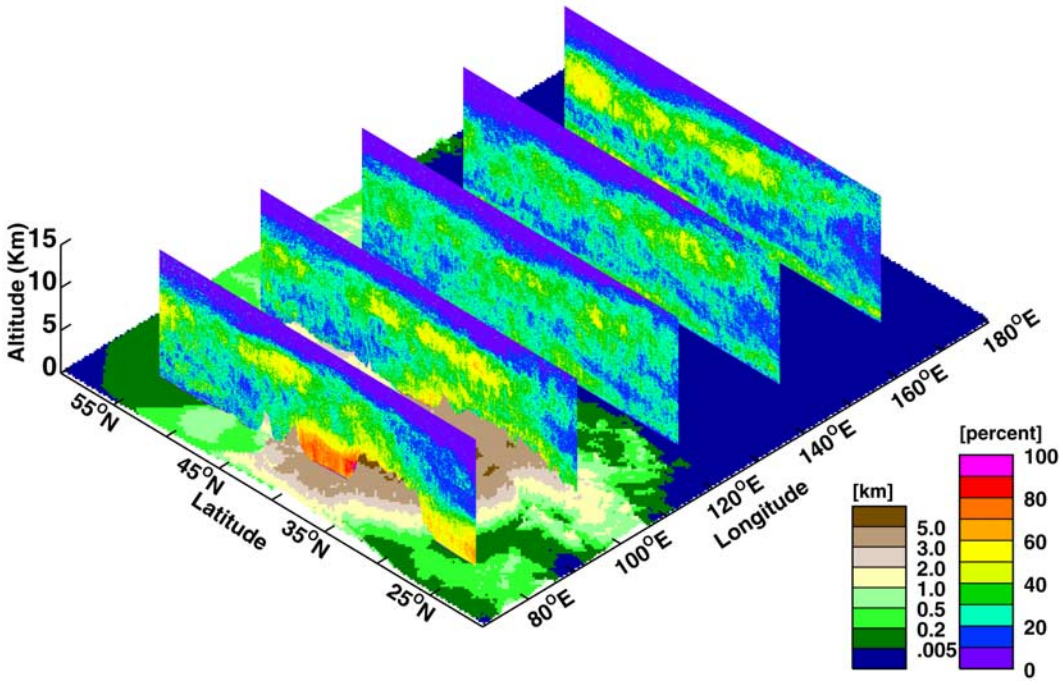

Figure 12. Dust event vertical structure from CALIPSO observations over the Taklamakan (80°E), Gobi (102°E), eastern China (124°E), Japan/China Yellow Sea (146°E), and the Pacific Ocean (168°E) superimposed on a regional map. Color scales on left represent topographical elevation, and those on the right represent dust event frequency of occurrence in percent.

Taklamakan (region A; Figure 10) the dust layer has a strong peak around 3 km and a weaker dust layer at 9 km. Such separation leads to the creation of a well-defined aerosol vertical structure that can be transported over long distances. The selected areas in the Gobi (region B) are associated with smaller dust loads in the lower altitudes but show a peak around 9 km, which is similar to that in the Taklamakan region. The vertical profile calculated for the ocean area (region C) shows strong peaks between 9 and 11 km for both wavelengths, which are likely due to long-range transport from the dust source regions. In Figure 14, the high dust aerosol extinction coefficients over the lower troposphere (below 2 km) of region C suggest that dust transport in the boundary layer was also significant during PACDEX.

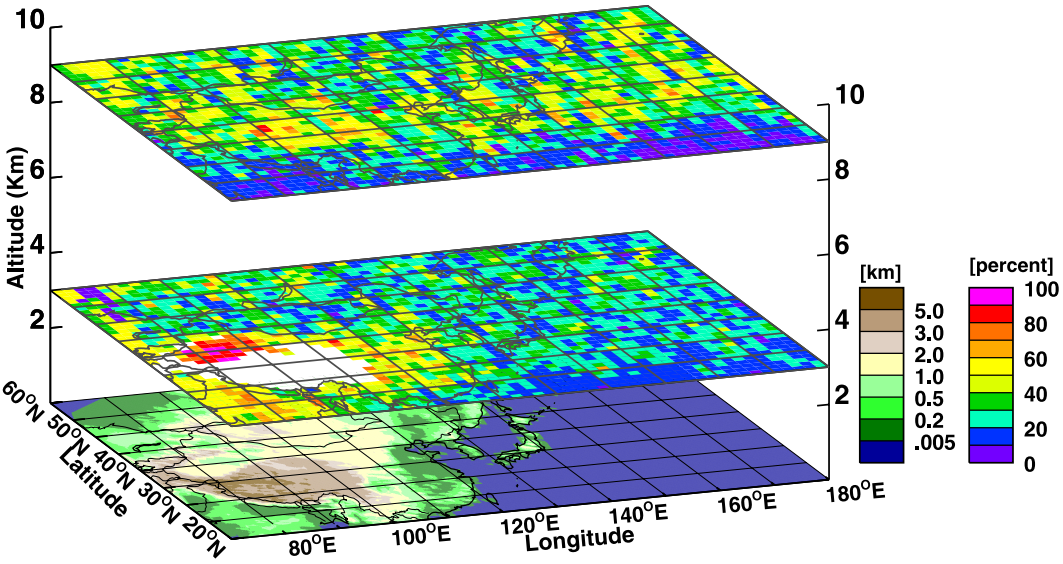

Figure 13. Horizontal distribution of dust event frequency of occurrence over eastern Asia and adjacent Pacific Ocean determined from CALIPSO measurements near the surface, at 3 km, and at 9 km. Color scales on the left represent topographical elevation, and those on the right represent dust event frequency of occurrence in percent.

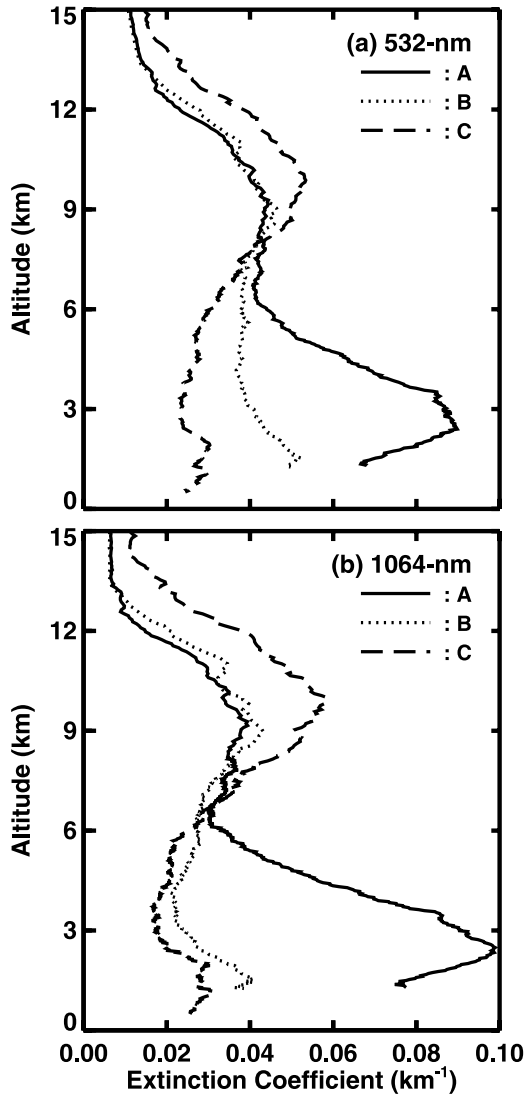

Figure 14. Vertical profiles of regionally averaged dust aerosol extinction coefficients (unit is km^{-1}) derived from CALIPSO for selected regions: (a) 532 nm and (b) 1064 nm.

[21] Figure 15 shows vertical profiles of aerosol extinction coefficients measured by the MPL at SACOL. Strong aerosol extinction was observed from 1 to 3 km for both the nighttime and afternoon profiles. Additional minor peaks can be found at 8 km for the afternoon profile and at 9 km for nighttime profiles indicating high-altitude aerosol layers. The low-altitude peak is possibly due to locally generated aerosols, while the high-altitude maximum is most likely due to convectively lifted aerosols that originated at distant sources and subsequently were transported by horizontal upper air movement.

5. Conclusions and Discussions

[22] Dust generated in the Taklamakan and Gobi deserts and Asian pollution can become entrained and transported by westerly jets across eastern Asia, the Pacific Ocean, and may even reach North America. Dust plumes often pass through Pacific Ocean extratropical cloud systems, which are important climate regulators because of their large radiative cooling effect. The effect of this mixed dust-pollution plume on Pacific cloud systems and their associated radiative forcing is an unexplored, yet key factor for understanding climate change. In this study, case studies and statistical analyses document the long-range transport and vertical structure of Asian dust during the PACDEX period (March through May 2007), a season that is typically active for the development of dust events. The study combined CALIPSO lidar backscatter with polarization measurements, in situ MPL, and standard meteorological measurements, together with air mass back trajectory analysis to identify dust sources and transport paths. It showed that dust aerosols primarily originate near the Taklamakan and Gobi deserts and are then transported over eastern China and the Pacific Ocean. Over eastern China and the western Pacific Ocean, two-layer aerosol structures are often apparent, which may be associated with contributions from two major dust sources. This study demonstrated that dust layer vertical structure depends on the dust source and dust event intensity. The dust events are more frequent in the Taklamakan and surrounding area than in the Gobi region. However, floating dust events are predominant in the Taklamakan while more intensive dust storms are more common in the Gobi region. These differences are primarily due to different weather systems affecting the regions.

[23] The Taklamakan dust events are primarily induced by cold high-pressure systems, with cold air moving into the Tarim Basin from its east gate or from air moving over the

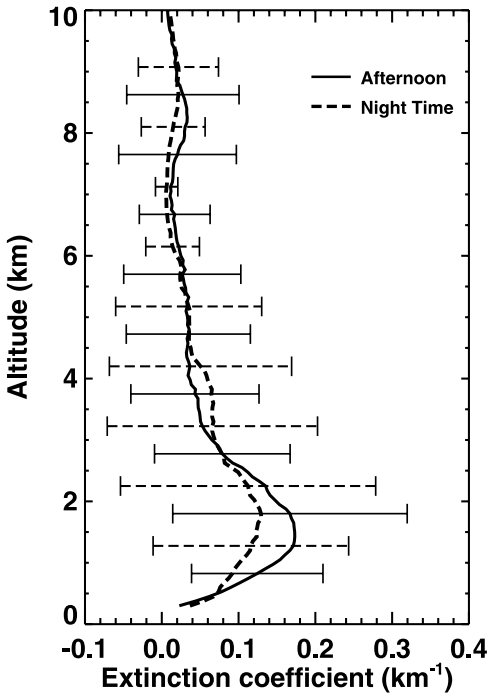

Figure 15. Mean vertical profile of MPL aerosol extinction coefficients (km^{-1}) for afternoon (1400–1600 local time) and nighttime (0200–0400 LT) with error bars indicating standard deviations computed from vertical bins of each profile.

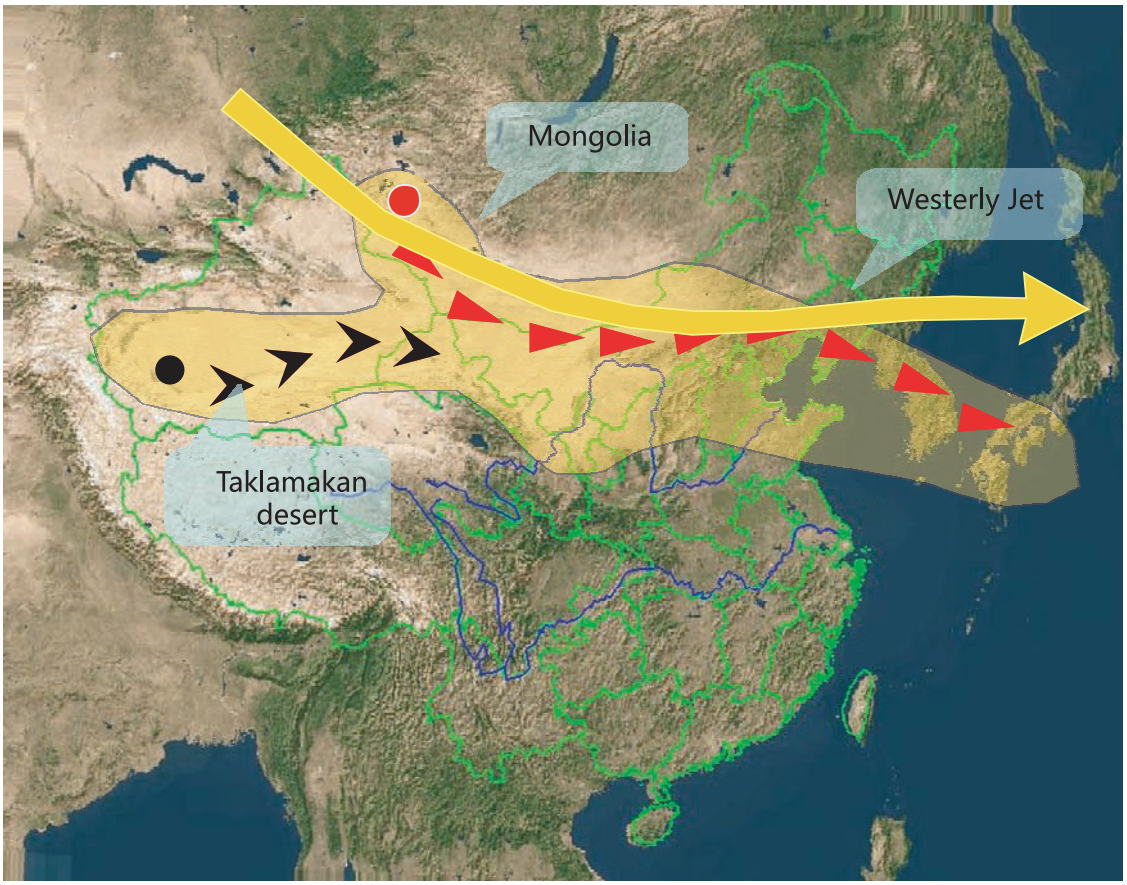

Figure 16. Illustration of major dust event paths observed during PACDEX. Black and red dots are sources of dust outbreaks, red arrows represent northwestern path, black arrows represent the western path, and the yellow line represents the jet flow at 500 hPa.

Tianshan Mountains and rushing down into the basin. Prior to the cold high-pressure systems moving into the basin, the ground temperatures are generally higher. This creates instability and intensifies cross ventilation leading to updrafts that transport sediments when wind speeds exceed 10 m/s. Because the areas to the north, west, and south of the Taklamakan desert (Tarim Basin) are surrounded by high mountains with average elevations of more than 5000 m dust transport is restricted at lower altitudes. On the basis of analyses of 1960–1999 meteorological data and a case study in 1986, *Sun* [2002] and *Sun et al.* [2001] found that the winds near the surface in the Tarim Basin are easterly or northeasterly, which suggests that the dust aerosols cannot move out of this area at an altitude below 5000 m. However, if the aerosols are lifted to a higher altitude, they can be transported long distances, to the Pacific Ocean and beyond, by westerly jets (*Sun et al.* [2001], also see the example in Figure 2). The vertical distributions of the CALIPSO backscattering/depolarization ratios indicate that nonspherically shaped dust aerosols floated from near the ground to about 10 km around the Taklamakan desert region. This suggests the possible long-range transport of dust aerosols entrained into the upper troposphere westerly jets at altitudes above 6 km.

[24] The Gobi dust events are generally caused by developing synoptic-scale cyclones. These dust events can be enhanced when a cyclone develops to a deeper frontal system and moves southeastward led by upper level jet flow. Using long-term climatological records of dust storms and meteorological data in China, *Sun et al.* [2001] concluded that mineral dust originating from the Gobi Desert could not be lifted to altitudes greater than 3 km. However, our results show that dust originating from the Gobi Desert can extend up to altitudes of 8 km. CALIPSO observations frequently detect a large depolarization ratio layer from near the ground to around 9 km. The vertical distribution of the layer with high scattering ratios shows good correspondence with the vertical distribution of the particle depolarization ratio. These results suggest that Gobi dust can be transported to Pacific Ocean within both the lower and upper troposphere.

[25] Figure 16 summarizes the major transit pathways of dust storms observed during PACDEX. There were 10 large-scale dust storms, 6 occurred in the Mongolia/Gobi Desert while the remainder occurred in the Taklamakan Desert (Tarim Basin). Because dust events are more frequent in the Taklamakan than in the Gobi region, the 4 dust storm cases only contribute 1.4% percent to the observations shown in Figure 10. Figure 16 illustrates how the dust from these storms spread to Mongolia, northern China, the Yellow Sea, the Korean Peninsula, southern Japan, and the Pacific Ocean southeast of Japan. The

Mongolia/Gobi Desert and Taklamakan Desert were identified as the major sources of dust. The major transfer paths are over northern China where dust clouds moved to the Pacific Ocean over southeast Japan, and from the west where the dust storms mainly affected the local area with heavy concentrations at low levels.

[26] The conclusions from this study are only based on satellite and surface measurements taken during the PACDEX (March–May 2007) field experiment and do not cover a sufficient time span to definitively conclude that the observed dust particle vertical distributions and long-range transport are predominant for the region. Long-term monitoring and analysis is necessary to determine the typical dust particle vertical distributions and transport mechanisms for the region. Further research should focus on combining CALIPSO measurements with other A-Train satellite measurements as well as measurements from aircraft and surface network/super sites.

[27] **Acknowledgments.** This research is supported by National Science Foundation of China under grants 40628005 and 40633017 and the NASA Science Mission Directorate through the CALIPSO Project and the Radiation Sciences Program. The CALIPSO data were obtained from the NASA Langley Atmospheric Science Data Center (ASDC).

References

Carlson, T. N., and S. G. Benjamin (1980), Radiative heating rates for Saharan dust, *J. Atmos. Sci.*, *37*(1), 193–213, doi:10.1175/1520-0469(1980)037<0193:RHRFSD>2.0.CO;2.

Claquin, T., M. Schulz, Y. J. Balkanski, and O. Boucher (1998), Uncertainties in assessing radiative forcing by mineral dust, *Tellus, Ser. B*, *50*, 491–505, doi:10.1034/j.1600-0889.1998.t01-2-00007.x.

DeMott, P. J., K. Sassen, M. R. Poellot, D. Baumgardner, D. C. Rogers, S. D. Brooks, A. J. Prenni, and S. M. Kreidenweis (2003), African dust aerosols as atmospheric ice nuclei, *Geophys. Res. Lett.*, *30*(14), 1732, doi:10.1029/2003GL017410.

Draxler, R. R. and G. D. Rolph (2003), HYSPLIT (Hybrid Single-Particle Lagrangian Integrated Trajectory) model, Air Resour. Lab., NOAA, Silver Spring, Md. (Available at http://www.arl.noaa.gov/ready/hysplit4.html)

Forster, P., et al. (2007), Changes in atmospheric constituents and in radiative forcing, in *Climate Change 2007: The Physical Science Basis—Contribution of Working Group I to the Fourth Assessment Report of the Intergovernmental Panel on Climate Change*, edited by S. Solomon et al., chap. 2, pp. 129–134, Cambridge Univ. Press, Cambridge, U. K.

Holben, B. N., et al. (1998), AERONET—A federated instrument network and data archive for aerosol characterization, *Remote Sens. Environ.*, *66*, 1–16, doi:10.1016/S0034-4257(98)00031-5.

Hu, Y., et al. (2006), A simple relation between depolarization and multiple scattering of water clouds and its application for lidar calibration, *Opt. Lett.*, *31*, 1809–1811, doi:10.1364/OL.31.001809.

Huang, J., P. Minnis, Y. Yi, Q. Tang, X. Wang, Y. Hu, Z. Liu, K. Ayers, C. Trepte, and D. Winker (2007), Summer dust aerosols detected from CALIPSO over the Tibetan Plateau, *Geophys. Res. Lett.*, *34*, L18805, doi:10.1029/2007GL029938.

Huang, J., et al. (2008), An overview of the Semi-Arid Climate and Environment Research Observatory over the Loess Plateau, *Adv. Atmos. Sci.*, *25*(6), 906–921, doi:10.1007/s00376-008-0906-7.

Husar, R. B., et al. (2001), Asian dust events of April 1998, *J. Geophys. Res.*, *106*(D16), 18,317–18,330, doi:10.1029/2000JD900788.

Iwasaka, Y., H. Minoura, and K. Nagaya (1983), The transport and spatial scale of Asian dust-storm clouds: A case study of the dust-storm event of April 1979, *Tellus, Ser. B*, *35*, 189–196.

Kwon, S. A., Y. Iwasaka, T. Shibata, and T. Sakai (1997), Vertical distribution of atmospheric particles and water vapor densities in the free troposphere: Lidar measurement in spring and summer in Nagoya, Japan, *Atmos. Environ.*, *31*, 1459–1465, doi:10.1016/S1352-2310(96)00310-X.

Liao, H., and J. H. Seinfeld (1998), Radiative forcing by mineral dust aerosols: Sensitivity to key variables, *J. Geophys. Res.*, *103*(D24), 31,637–31,645, doi:10.1029/1998JD200036.

Liu, D., Z. Wang, Z. Liu, D. Winker, and C. Trepte (2008), A height resolved global view of dust aerosols from the first year CALIPSO lidar measurements, *J. Geophys. Res.*, *113*, D16214, doi:10.1029/2007JD009776.

Liu, Z., N. Sugimoto, and T. Murayama (2002), Extinction-to-backscatter ratio of Asian dust observed with high-spectral-resolution lidar and Raman lidar, *Appl. Opt.*, *41*, 2760–2767, doi:10.1364/AO.41.002760.

Liu, Z., W. Hunt, M. Vaughan, C. Hostetler, M. McGill, K. Powell, D. Winker, and Y. Hu (2006), Estimating random errors due to shot noise in backscatter lidar observations, *Appl. Opt.*, *45*(18), 4437–4447, doi:10.1364/AO.45.004437.

Liu, Z., et al. (2008), CALIPSO lidar observations of optical properties of Saharan dust: A case study of long range transport, *J. Geophys. Res.*, *113*, D07207, doi:10.1029/2007JD008878.

Matsuki, A., et al. (2003), Seasonal dependence of the long-range transport and vertical distribution of free tropospheric aerosols over east Asia: On the basis of aircraft and lidar measurements and isentropic trajectory analysis, *J. Geophys. Res.*, *108*(D23), 8663, doi:10.1029/2002JD003266.

Meloni, D., A. D. Sarra, T. D. Iotio, and G. Fiocco (2005), Influence of the vertical profile of Saharan dust on the visible direct radiative forcing, *J. Quant. Spectrosc. Radiat. Transfer*, *93*, 397–413.

Minnis, P. and S. K. Cox (1978), Magnitude of the radiative effects of the Sahara dust layer, *Atmos. Sci. Pap.*, *283*, 111 pp., Colo. State Univ., Fort Collins.

Murayama, T., et al. (2001), Ground-based network observation of Asian dust events of April 1998 in east Asia, *J. Geophys. Res.*, *106*(D16), 18,345–18,360, doi:10.1029/2000JD900554.

Murayama, T., et al. (2003), An intercomparison of lidar-derived aerosol optical properties with airborne measurements near Tokyo during ACE-Asia, *J. Geophys. Res.*, *108*(D23), 8651, doi:10.1029/2002JD003259.

Murayama, T., D. Muller, K. Wada, A. Shimizu, M. Sekiguchi, and T. Tsukamoto (2004), Characterization of Asian dust and Siberian smoke with multi-wavelength Raman lidar over Tokyo, Japan in spring 2003, *Geophys. Res. Lett.*, *31*, L23103, doi:10.1029/2004GL021105.

Natsagdorj, L., D. Jugder, and Y. S. Chung (2003), Analysis of dust storms observed in Mongolia during 1937–1999, *Atmos. Environ.*, *37*, 1401–1411, doi:10.1016/S1352-2310(02)01023-3.

Ramanathan, V., et al. (2001), Indian Ocean experiment: An integrated analysis of the climate forcing and effects of the great Indo-Asian haze, *J. Geophys. Res.*, *106*(D22), 28,371–28,398, doi:10.1029/2001JD900133.

Sasano, Y. (1996), Tropospheric aerosol extinction coefficient profiles derived from scanning lidar measurements over Tsukuba, Japan from 1990 to 1993, *Appl. Opt.*, *35*(24), 4941–4952.

Sassen, K. (2002), Indirect climate forcing over the western US from Asian dust storms, *Geophys. Res. Lett.*, *29*(10), 1465, doi:10.1029/2001GL014051.

Satheesh, S. K. (2002), Aerosol radiative forcing over land: Effect of surface and cloud reflection, *Ann. Geophys.*, *20*(12), 2105–2109.

Satheesh, S. K., and V. Ramanathan (2000), Large difference in tropical aerosol forcing at the top of the atmosphere and Earth's surface, *Nature*, *405*, 60–63, doi:10.1038/35011039.

Shimizu, A., N. Sugimoto, I. Matsui, K. Arao, I. Uno, T. Murayama, N. Kagawa, K. Aoki, A. Uchiyama, and A. Yamazaki (2004), Continuous observations of Asian dust 16 and other aerosols by polarization lidars in China and Japan during ACE-Asia, *J. Geophys. Res.*, *109*, D19S17, doi:10.1029/2002JD003253.

Sun, J. (2002), Provenance of loess material and formation of loess deposits on the Chinese loess plateau, *Earth Planet. Sci. Lett.*, *203*, 845–859, doi:10.1016/S0012-821X(02)00921-4.

Sun, J., M. Zhang, and T. Liu (2001), Spatial and temporal characteristics of dust storms in China and its surrounding regions, 1960–1999: Relations to source area and climate, *J. Geophys. Res.*, *106*, 10,325–10,333, doi:10.1029/2000JD900665.

Tsunematsu, N., K. Kai, and T. Matsumoto (2005), The influence of synoptic-scale air flow and local circulation on the dust layer height in the north of the Taklimakan Desert, *Water Air Soil Pollut. Focus*, *5*, 175–193, doi:10.1007/s11267-005-0734-z.

Uno, I., H. Amano, S. Emori, K. Kinoshita, I. Matsui, and N. Sugimoto (2001), Trans- Pacific yellow sand transport observed in April 1998: A numerical simulation, *J. Geophys. Res.*, *106*(D16), 18,331–18,344, doi:10.1029/2000JD900748.

Uno, I., K. Yumimoto, A. Shimizu, Y. Hara, N. Sugimoto, Z. Wang, Z. Liu, and D. M. Winker (2008), 3D structure of Asian dust transport revealed by CALIPSO lidar and a 4DVAR dust model, *Geophys. Res. Lett.*, *35*, L06803, doi:10.1029/2007GL032329.

Vaughan, M., et al. (2004), Fully automated analysis of space-based lidar data: An overview of the CALIPSO retrieval algorithms and data products, *Proc. SPIE Int. Soc. Opt. Eng.*, *5575*, 16–30, doi:10.1117/12.572024.

Wang, S., J. Wang, Z. Zhou, and K. Shang (2005), Regional characteristics of three kinds of dust storm events in China, *Atmos. Environ.*, *39*, 509–520, doi:10.1016/j.atmosenv.2004.09.033.

Welton, E. J., J. R. Campbell, J. D. Spinhirne, and V. S. Scott (2001), Global monitoring of clouds and aerosols using a network of micropulse

lidar systems, *Proc. SPIE Int. Soc. Opt. Eng.*, *4153*, 151–158, doi:10.1117/12.417040.

Winker, D. M., W. H. Hunt, and M. J. McGill (2007), Initial performance assessment of CALIOP, *Geophys. Res. Lett.*, *34*, L19803, doi:10.1029/2007GL030135.

Zhang, X. Y., R. Arimoto, and Z. S. An (1997), Dust emission from Chinese desert sources linked to variations in atmospheric circulation, *J. Geophys. Res.*, *102*(D23), 28,041–28,044, doi:10.1029/97JD02300.

Zhou, J., G. Yu, C. Jin, F. Qi, D. Liu, H. Hu, Z. Gong, G. Shi, T. Nakajima, and T. Takamura (2002), Lidar observations of Asian dust over Hefei, China in Spring 2000, *J. Geophys. Res.*, *107*(D15), 4252, doi:10.1029/2001JD000802.

Zhu, A., V. Ramanathan, F. Li, and D. Kim (2007), Dust plumes over the Pacific, Indian, and Atlantic oceans: Climatology and radiative impact, *J. Geophys. Res.*, *112*, D16208, doi:10.1029/2007JD008427.

J. K. Ayers and Y. Yi, Science Systems and Applications Incorporated, Hampton, VA 23666, USA.

B. Chen, J. Huang, and Z. Huang, College of Atmospheric Science, Lanzhou University, Lanzhou 730000, China. (hjp@lzu.edu.cn)

Z. Liu, National Institute of Aerospace, Hampton, VA 23666, USA.

P. Minnis, NASA Langley Research Center, Hampton, VA 23666, USA.

Q. Zhao, Gansu Meteorological Bureau, Lanzhou 730000, China.